HHS Public Access

Author manuscript

Sci Transl Med. Author manuscript; available in PMC 2016 July 27.

Published in final edited form as:

Sci Transl Med. 2016 March 30; 8(332): 332ra42. doi:10.1126/scitranslmed.aaf1164.

Somatic *PIK3CA* mutations as a driver of sporadic venous malformations

Pau Castel[1], **F. Javier Carmona**[1], **Joaquim Grego-Bessa**[2], **Michael F. Berger**[1,3], **Agnès Viale**[4], **Kathryn V. Anderson**[2], **Silvia Bague**[5], **Maurizio Scaltriti**[1,3], **Cristina R. Antonescu**[3], **Eulàlia Baselga**[6], and **José Baselga**[1,7,*]

[1]Human Oncology and Pathogenesis Program (HOPP), Memorial Sloan Kettering Cancer Center, 1275 York Avenue, New York, NY 10065, USA

[2]Developmental Biology Program, Sloan Kettering Institute, New York, NY 10065, USA

[3]Department of Pathology, Memorial Sloan Kettering Cancer Center, New York, NY 10065, USA

[4]Genomics Core Laboratory, Memorial Sloan Kettering Cancer Center, New York, NY 10065, USA

[5]Department of Pathology, Hospital de la Santa Creu i Sant Pau, 167 Sant Antoni M. Claret, Barcelona 08025, Spain

[6]Department of Dermatology, Hospital de la Santa Creu i Sant Pau, Barcelona 08025, Spain

[7]Department of Medicine, Memorial Sloan Kettering Cancer Center, New York, NY 10065, USA

Abstract

Venous malformations (VM) are vascular malformations characterized by enlarged and distorted blood vessel channels. VM grow over time and cause substantial morbidity because of disfigurement, bleeding, and pain, representing a clinical challenge in the absence of effective treatments (Nguyen *et al.*, 2014; Uebelhoer *et al.*, 2012). Somatic mutations may act as drivers of these lesions, as suggested by the identification of *TEK* mutations in a proportion of VM (Limaye *et al.*, 2009). We report that activating *PIK3CA* mutations gives rise to sporadic VM in mice,

*Corresponding author. baselgaj@mskcc.org.

SUPPLEMENTARY MATERIALS

www.sciencetranslationalmedicine.org/cgi/content/full/8/332/332ra42/DC1 Materials and Methods

Fig. S1. Histologic characterization of *PIK3CA*$^{\text{Sprr2f-Cre}}$ mice.

Fig. S2. *PIK3CA* mutation in ECs.

Fig. S3. Histologic characterization of *PIK3CA*$^{\text{CAG-CreER}}$ mice.

Fig. S4. Histologic characterization of *PIK3CA*$^{\text{UBC-CreER}}$ mice.

Fig. S5. Cell proliferation in mouse VM with or without in vivo treatments.

Fig. S6. Treatment of VM with PI3K inhibitors.

Fig. S7. Histological assessment of *PIK3CA*$^{\text{Tie2-Cre}}$ embryos.

Table S1. Clinical features and genomic findings in VM patients. Table S2. Bait sequences used for *TEK* targeted sequencing.

Author contributions: P.C. and J.B. conceived the project. P.C., M.S., K.V.A., E.B., and J.B. supervised the research. P.C., F.J.C., and J.G.-B. performed the in vitro and in vivo experiments. C.R.A. reviewed the human and mice cases. C.R.A., S.B., and E.B. provided patients' samples. M.F.B. and A.V. supervised and analyzed the sequencing. P.C. prepared the figures. P.C., F.J.C., E.B., and J.B. wrote the manuscript.

Competing interests: J.B. has consulted for Novartis Pharmaceuticals and serves on the board of Infinity Pharmaceuticals. The authors (P.C., E.B., and J.B.) have applied for a patent for the use of PI3K inhibitors for the treatment of vascular malformations.

Data and materials availability: MSK-IMPACT raw sequencing data are available upon request. For the reagents, please contact the corresponding author.

which closely resemble the histology of the human disease. Furthermore, we identified mutations in *PIK3CA* and related genes of the PI3K (phosphatidylinositol 3-kinase)/AKT pathway in about 30% of human VM that lack *TEK* alterations. *PIK3CA* mutations promote downstream signaling and proliferation in endothelial cells and impair normal vasculogenesis in embryonic development. We successfully treated VM in mouse models using pharmacological inhibitors of PI3Kα administered either systemically or topically. This study elucidates the etiology of a proportion of VM and proposes a therapeutic approach for this disease.

INTRODUCTION

Venous malformations (VM) [Online Mendelian Inheritance in Man (OMIM) #600195] are the most frequent form of vascular malformation and are characterized by the presence of a single endothelial layer forming distended blood vessels of variable diameter that are surrounded by a disorganized mural cell layer containing both smooth muscle cells and pericytes (*1*, *2*). Sporadic VM are particularly evident when they involve skin or mucosae. These lesions grow over time, causing substantial morbidity such as disfigurement, bleeding, and pain. They may also affect other tissues including muscles, joints, or the intestine (*3*). Furthermore, they represent a clinical challenge because of the lack of effective treatments, although some patients derive limited benefits from surgery or sclerotherapy (*4*, *5*). Currently, there are no approved pharmacological treatments for these lesions that often tend to recur after conventional therapy.

Previous studies in sporadic VM have identified activating somatic mutations in the gene coding for the endothelial-specific tyrosine kinase receptor *TEK* (TIE2) in almost half of the cases analyzed (*6*, *7*). Activating mutations in *TEK* result in enhanced activation of the downstream PI3K (phosphatidylinositol 3-kinase)/AKT and MAPK (mitogen-activated protein kinase) pathways (*8*–*11*) and have been shown to promote the growth of human umbilical vein endothelial cells (HUVECs) in xenograft assays (*11*), deregulate the expression of genes involved in vascular development (*12*), compromise the endothelial cell (EC) monolayer as a result of the loss of fibronectin (*13*), and decrease the expression of the mural cell attractant PDGFB (platelet-derived growth factor, β polypeptide) (*12*). However, in a large proportion of VM that do not harbor mutations in *TEK*, the underlying pathogenesis remains unknown.

The PI3K pathway is a central regulator of cell survival, growth, and metabolism (*14*), and its deregulation as a result of genetic or epigenetic perturbations is observed in a variety of human tumors and overgrowth syndromes (*15*, *16*). PI3K is regulated by virtually all receptor tyrosine kinases, including TIE2, and mediates the phosphorylation of phosphatidylinositol 4,5-biphosphate, giving rise to the second messenger phosphatidylinositol 3,4,5-trisphosphate that triggers downstream signaling. AKT and mTOR (mammalian target of rapamycin) are two well-studied effectors of the PI3K pathway and are responsible for the cellular phenotypes such as cell cycle progression, proliferation, anabolism, and others (*14*). PI3K also plays a critical role in vascular homeostasis, and this pathway is essential for angiogenesis and maintenance of the mature endothelium (*17*, *18*).

Hotspot mutations in *PIK3CA*, the gene encoding for the catalytic p110α subunit of PI3K, cause pathway hyperactivation resulting in cellular transformation and uncontrolled growth in epithelial and mesenchymal cells (*15*). This aberrant PI3K/AKT signaling is associated with overgrowth syndromes that are often accompanied by different types of vascular malformations including lymphatic, venous, and arteriovenous malformations (*19*), as well as isolated lymphatic malformations (*20*).

We report the existence of gain-of-function mutations in the PI3K/ AKT pathway in clinical specimens of isolated sporadic VM and provide a genetically engineered mouse model (GEMM) of this disease. The presence of *PIK3CA* mutations in sporadic VM, together with the observation that these mutations are mutually exclusive with *TEK* mutations, suggests that VM may be defined as a disease state characterized by the presence of somatic activating mutations in the TIE2-PI3K-AKT axis. Together, these findings could result in the development of efficacious therapies for this challenging disease and could contribute to a genomically based classification of vascular lesions.

RESULTS

PIK3CA$^{Sprr2f\text{-}Cre}$ mice develop spinal and cutaneous VM

An unexpected finding pointed us toward the critical role of PI3K in the pathogenesis of VM. We were originally interested in studying the role of *PIK3CA*, the gene encoding the catalytic p110α subunit of PI3K (PI3Kα), in uterine cancer, which is characterized by the presence of these mutations in approximately half of the cases (*21*). To investigate the role of *PIK3CA* oncogenicity in this disease, we took advantage of the previously reported transgenic mouse strain LoxP-STOP-LoxP(LSL)–*PIK3CA*^{H1047R}, which allows the expression of the activating *PIK3CA* mutation H1047R in a tissue-specific manner using the Cre-loxP technology upon removal of the floxed synthetic transcriptional/translational STOP cassette (*22*). These animals were crossed with the Sprr2f-Cre strain, shown to drive Cre recombinase expression in both luminal and glandular uterine epithelial cells (fig. S1A) (*23*). Unexpectedly, although *PIK3CA*$^{Sprr2f\text{-}WT}$ mice were viable and normal, *PIK3CA*$^{Sprr2f\text{-}Cre}$ littermates exhibited hindlimb paralysis at an early age (4 to 10 weeks) (Fig. 1A). Because this phenotype was observed in both males and females, we decided to further explore the pathologic events underlying this phenotype. Histologic examination revealed lesions in the spinal cord resembling human vascular malformations that were not present in wild-type animals (Fig. 1B). Specifically, these abnormalities showed dilated “cavernous” vascular spaces with extensive blood pools and hemorrhage involving both white and gray matter.

We further examined the spinal lesions in *PIK3CA*$^{Sprr2f\text{-}Cre}$ mice injected intravenously with gold nanoparticles, using the in vivo x-ray computed tomography imaging to confirm the presence of hyperdense lesions in the spine. These vascular lesions were present in animals with both advanced and milder phenotypes but not in wild-type littermates (Fig. 1C) and showed slow blood flow and extravasation, radiological features of vascular malformations of the spine (*24*). The abnormal vascular channels, represented by cavernous spaces and capillary proliferation, were consistent with a diagnosis of VM according to the current classification of the International Society for the Study of Vascular Anomalies (*25*). Among the observed alterations, cutaneous VM were the most frequent, exhibiting high penetrance

in the *PIK3CA*$^{Sprr2f\text{-}Cre}$ mice (about 90%) (Fig. 1D). Microscopically, the skin lesions resembled human VM with positivity for CD31 (Fig. 1E and fig. S1B) and Perl's Prussian blue staining (Fig. 1F), indicative of EC lining and hemosiderin deposition, respectively.

To further characterize the observed lesions, we stained our mouse VM for both glucose transporter1 (GLUT-1) and Wilms tumor1 (WT-1), which are immunophenotyping markers of infantile hemangioma (IH), a different vascular disease with a distinct natural history that responds to the β-blocker propranolol (*26–28*). Both types of staining were negative in mouse VM samples as compared to positive controls from human IH specimens and mouse tissue (fig. S1, C and D). Lymphatic malformations, which can histologically resemble VM, can also harbor *PIK3R1* and *PIK3CA* mutations (*29*). In fact, mice with a knockout of *PIK3R1*, encoding the PI3K regulatory subunits p85α, p55α, and p50α, have defects in normal lymphangiogenesis and develop lymphatic malformations in the intestines and skin (*30*).

Thus, to assess whether our VM model might exhibit a substantial lymphatic component, we stained for the lymphatic-specific markers lymphatic vessel endothelial hyaluronan receptor 1 (LYVE-1) (*31*) and prospero homeobox 1 (PROX-1) (*32*). Our IHC staining with these lymphatic markers did not detect any relevant reactivity in the areas comprising the malformation, indicating that these lesions are entirely VM (fig. S1, E and F).

We hypothesized that the Sprr2f-Cre strain drives the expression of the Cre recombinase in mature or precursor ECs, in addition to the reported endometrial epithelial cells. Thus, we crossed the LSL-LacZ reporter strain with the Sprr2f-Cre mouse and performed β-galactosidase staining in spinal sections. In LacZ$^{Sprr2f\text{-}Cre}$ sections, we detected discrete positive cells resembling ECs that were sparsely distributed within the white and gray matter of the spinal cord (fig. S1G). Because of technical constraints, we were not able to obtain double staining for LacZ and CD31. However, double immunofluorescence staining against Cre and CD31 on VM from the Sprr2f-Cre mice confirmed the presence of Cre recombinase in the CD31-positive lesions that explain the vascular phenotype observed in these mice (fig. S1H).

PIK3CA activating mutation affects normal ECs

Analogous to recent studies (*11*), we transduced primary human skin ECs with retrovirus encoding the *PIK3CA* wild type or H1047R variants to study the cellular mechanisms by which *PIK3CA* mutations might alter EC function. *PIK3CA*^{H1047R} mutant cells exhibited amplified downstream PI3K/AKT/mTOR signaling with increased phosphorylation of AKT at S^{473} and T^{308}, and the mTOR downstream targets S6 kinase at T^{389} and ribosomal S6 protein at $S^{235/6}$ and $S^{240/4}$ (Fig. 2A). We undertook tube formation assays to assess the ability of these cells to form a normal capillary network in a three-dimensional matrix, an approach widely used to assess the normal function of EC (*33*). *PIK3CA*^{H1047R} mutant cells formed aberrant EC clusters, as opposed to their wild-type counterparts, which generated normal vascular tubes in vitro (Fig. 2B). We further confirmed these results using HUVECs infected with *PIK3CA* wild type and the H1047R mutant, which recapitulated the increased PI3K/AKT signaling (fig. S2A) and aberrant tube formation in vitro (fig. S2B). Because PI3K regulates cell proliferation (*18*), we tested the proliferation ratio of our primary cells in

vitro using 5-ethynyl-2′-deoxyuridine (EdU) incorporation assays and found that the mutant cells exhibited a slightly higher, but reproducible, proliferation rate as compared with wild-type cells and empty vector controls, which was reversed upon treatment with a PI3Ka inhibitor (Fig. 2C) in a dose-dependent manner (fig. S2, C and D).

ECs, which are key players in the development of vascular malformations, create a pathological niche that involves the mural cell compartment, probably in part as a result of aberrant cytokine secretion (*12*, *34*). To test the impact of the *PIK3CA* activating mutation H1047R on the secretion of angiogenic factors, we performed antibody arrays in our primary ECs carrying wild-type *PIK3CA* or the H1047R mutation. We found that angiopoietin-2 (ANG2) protein expression was decreased in *PIK3CA*^{H1047R} but not in the *PIK3CA*^{WT} or control cells (fig. S2E).

Because ANG2 is a cytokine that is regulated by forkhead O (FOXO) transcription factors downstream of the PI3K/AKT pathway, inhibits blood vessel leakage (*35*), and plays a role in the pathogenesis of lymphatic malformations and VM (*12*, *20*, *36*), we sought to confirm whether our primary ECs displayed decreased expression of ANG2. Consistently, *PIK3CA*^{H1047R} mutant ECs had lower expression of *ANGPT2* mRNA and secreted ANG2 protein compared to *PIK3CA*^{WT} cells and empty vector controls (fig. S2F). Next, we treated *PIK3CA*^{H1047R} ECs with the different inhibitors of the PI3K/AKT/mTOR pathway, namely, BYL719 (PI3Kα), MK2206 (AKT), and everolimus (mTOR). We observed that both PI3Kα and AKT inhibitors were able to rescue the mRNA and protein expression of ANG2, but the mTOR inhibitor everolimus was not (fig. S2F). These results are in agreement with the previous evidence describing this secretory phenotype in VM, where PDGFB and ANG2 are down-regulated in *TEK* mutant ECs (*12*).

Human VM harbor *PIK3CA* mutations

Next, to ascertain whether the same genetic alterations triggering the phenotype in our mouse and cellular models were also present in the human condition, we examined clinical specimens from 32 patients, mainly adults (median age, 36 years), diagnosed with VM (table S1). Patients diagnosed with VM at our institution, a cancer center, mainly presented with deep-seated and infiltrative masses in the skeletal muscle (53% of the cases were intramuscular, 34% involved skin, and 13% were in other locations) (table S1). Histologically, these lesions displayed a mixed pattern of vascular proliferation, including thick-walled malformed vessels, cavernous spaces filled with erythrocytes, and capillary areas (Fig. 2D), and these were radiologically detected by routine magnetic resonance imaging (MRI) scans (Fig. 2E). We analyzed these VM by targeted exome sequencing of 341 cancer-related genes using the MSK-IMPACT (Memorial Sloan Kettering–Integrated Mutation Profiling of Actionable Cancer Targets) assay (*37*) developed at our institution, yielding a median coverage of 588X. This assay was complemented with the next-generation deep sequencing targeted to the *TEK* locus (table S2). Deep sequencing detected *PIK3CA* mutations in 25% (8 of 32) of cases in previously described (*38*) hotspots encoding for the gain-of-function mutations H1047R (3 of 32) and E542K (3 of 32) with an allele frequency ranging from 3 to 15% (Fig. 2F and fig. S2G). We also identified two other mutations in *PIK3CA*, coding for C420R and I143V. In addition, we found gain-of-function mutations in

other genes related to the PI3K pathway, such as *AKT2*, *AKT3*, and *IRS2*, resulting in an overall frequency of about 30% of mutations in the PI3K/AKT pathway (Fig. 2G and table S1). Because it was impossible to asses copy number variations in our cohort as a result of low cellularity and considering that amplification of *PIK3CA* and loss of *PTEN* are two common alterations of the PI3K pathway in human cancer, we performed fluorescence in situ hybridization analysis in all the VM patient samples sequenced. We did not find any amplification of *PIK3CA* or deletion of *PTEN* in any of the samples analyzed (fig. S2H). Furthermore, we found isolated mutations in genes involved in the MAPK pathway (*GNAQ*, *NF1*, *MAP2K1*, and *MAP3K1*) in 13% of the cases (Fig. 2G).

Previously described mutations in the tyrosine kinase receptor *TEK* (*6*, *7*) were found in 35% of the patients of our cohort, with allele frequencies ranging from 4 to 15%. These mutations were mutually exclusive with the mutations in the PI3K pathway, with the exception of one case (Fig. 2H). Considering that in ECs, the TIE2 receptor, encoded by *TEK*, is immediately upstream from PI3K and signals via PI3K itself (*9*, *13*, *39*), VM may be defined as a disease state characterized by the presence of somatic activating mutations in the TIE2-PI3K-AKT axis.

We were not able to detect any mutation in 5 of the 32 samples analyzed (table S1). This could be a result of low mutation allele frequency that is below the detection limit of our assay, the presence of a mutation that is not represented in our MSK-IMPACT assay, or a non-genetic etiology.

Ubiquitous expression of *PIK3CA*^{H1047R} spontaneously induces VM in mice

We hypothesized that the cell of origin giving rise to VM might be particularly sensitive to oncogenic *PIK3CA* transformation. Thus, we generated *PIK3CA*$^{CAG\text{-}CreER}$ mice, in which the *PIK3CA*^{H1047R} allele is ubiquitously expressed upon tamoxifen administration (fig. S3A) (*40*). Six- to eight-week-old mice fed with tamoxifen rapidly developed cutaneous VM with 100% penetrance compared to their *PIK3CA*^{WT} littermates (Fig. 3A). Histologic assessment confirmed a combined capillary and cavernous phenotype exhibiting dilated blood channels filled with erythrocytes (Fig. 3B) and immunoreactivity for CD31 (Fig. 3C) and phosphorylated AKT (S^{473}), a surrogate marker of PI3K activation (Fig. 3D).

Similar to human VM, murine vascular lesions from the *PIK3CA*$^{CAG\text{-}CreER}$ mice were negative for GLUT-1, WT-1, LYVE-1, and PROX-1 (fig. S3, B to E) and contained high amounts of hemosiderin deposition (Fig. 3E). Although the skin phenotype was readily evident, additional lesions were observed at necropsy at multiple sites, including mesentery, genitourinary tract, kidney, and retina (Fig. 3F), with no apparent difference in the incidence by anatomic site. Histological analyses of these lesions revealed large spaces filled with blood and lined by flattened ECs, with a similar immunophenotype, positive for CD31 and Prussian blue staining (Fig. 3, G and H).

We confirmed our findings using the UBC-CreER strain, another transgenic strain in which the ubiquitin C promoter drives the expression of a tamoxifen-inducible Cre recombinase in all the cells of the organism (fig. S4) (*41*). Consistently, our results indicated that upon

ubiquitous expression of the oncogenic *PIK3CA* transgene, the cell of origin for VM might be more sensitive to transformation than other cell types, resulting in the genesis of VM.

To test whether the formation of VM in our mouse model results, at least in part, from increased proliferation caused by hyperactive PI3K signaling (*42*, *43*), we measured 5-bromo-2′-deoxyuridine (BrdU) incorporation and Ki-67 staining in both *PIK3CA*^{WT} and *PIK3CA*$^{CAG\text{-}CreER}$ littermates. Whereas normal blood vessels were negative for BrdU incorporation as a consequence of EC quiescence (*44*), VM displayed a marked increase in proliferative cells (Fig. 3, I and J). In agreement with the BrdU data, Ki-67 positivity was found in our VM (fig. S5, A and B). We cannot rule out whether the proliferative enhancement observed is caused by the direct effect of the *PIK3CA* mutant allele or a result of autocrine and/or paracrine signaling from proliferating ECs, which plays an important role in the complex development of human VM (*12, 45*). At the morphological level, quantification of the lumen diameter from normal blood vessels and VM revealed a 10-fold increase in the size of these structures in VM samples (Fig. 3K).

PI3K inhibitors are effective in the treatment of *PIK3CA*-induced VM

The presence of oncogenic *PIK3CA* mutations in human specimens of VM, together with the observed phenotypes in mice, prompted us to evaluate the full growth potential of these lesions, despite the fact that they are considered to be vascular malformations. To this end, we injected *PIK3CA*$^{CAG\text{-}CreER}$ VM cells into recipient immunocompromised nude mice. These cells formed highly vascularized and proliferative masses a few weeks after injection, with a histology and appearance highly resembling that of the original lesions (Fig. 4A). Although VM do not have metastatic potential in patients, our finding that they may be successfully transplanted and grown in animals suggests that these lesions display some tumorigenic behaviors and highlight the fine line between malignant and benign tumors in some cases. Allotransplanted VM formed new cystic structures that contained blood and exhibited intravascular coagulopathy, as measured by the increased concentration of D-dimers in plasma (Fig. 4B), a useful tool for the differential diagnosis of VM in human patients (*46*).

Of clinical relevance, the presence of activating *PIK3CA* mutations in VM opens the door for the treatment of this condition with PI3Kα inhibitors, currently under clinical development for several cancer indications (*47*). Treatment of VM with the PI3Kα selective inhibitor BYL719 resulted in a marked response as measured by a decrease in VM volume (Fig. 4C), reduced proliferation, and increased apoptosis (Fig. 4D and fig. S5C). On the contrary, treatment with the β-adrenergic antagonist propranolol, an active agent against IH (*28*), did not yield any effect (Fig. 4, E and F, and fig. S5D). In support of the role of the aberrant activation of the PI3K/mTOR pathway in VM, treatment with the mTOR inhibitor everolimus (*48*, *49*) partially decreased VM size and proliferation in a similar fashion as PI3K inhibition, although it did not increase apoptosis (Fig. 4, E and F, and fig. S5D).

As mentioned above, VM may be defined as a disease characterized by the presence of somatic activating mutations in the TIE2-PI3K-AKT axis (Fig. 2, G and H). Because the TIE2 receptor, encoded by *TEK*, is immediately upstream from PI3K and signals via PI3K itself, we postulated that treatment with PI3K inhibitors might also be efficacious in VM

harboring *TEK* mutations. Indeed, treatment of HUVECs stably expressing the *TEK* mutation L914F with the PI3Kα inhibitor BYL719 decreased the amount of phosphorylated AKT (T^{308} and S^{473}) (fig. S6A), suggesting that PI3K inhibitors may be efficacious for VM with either *PIK3CA* or *TEK* mutations.

Given that a large number of VM are detected in the skin or superficial tissues, together with the substantial toxicity of systemic administration of PI3K inhibitors in patients (*50*), we wondered whether the topical application of PI3K inhibitors might be of therapeutic interest in this context. To this end, we formulated two different cream preparations containing the PI3Kα inhibitor BYL719 at 1% (w/w): one preparation with the inhibitor dispersed directly into the cream base and another one with the inhibitor presolubilized in dimethyl sulfoxide. Topical administration of the PI3Kα inhibitor using these two different cream formulas achieved a rapid and sustained regression of skin lesions (Fig. 4G and fig. S6B). Together, our results indicate that VM have tumorigenic growth potential as evidenced by their ability to engraft in nude mice and that the treatment with PI3K inhibitors either systemically or locally is a suitable pharmacological approach to control the disease.

Expression of mutant *PIK3CA* impairs normal vasculogenesis

VM may occur as a result of defects during angiogenesis, a process in which PI3Kα is actively involved (*17*, *18*, *51*). To explore the biological relevance of PI3K hyperactivation specifically in blood vessels, we crossed *PIK3CA*^{H1047R} mice with the Tie2-Cre strain (*52*), which drives the expression of the transgene in ECs (fig. S7A). *PIK3CA*$^{Tie2\text{-}Cre}$ mice were not viable because of early embryonic lethality [embryonic day 10 (E10)] resulting from vascular defects (Fig. 5A). CD31 staining of coronal sections revealed dilated blood vessels and vascular anomalies (Fig. 5B, upper panel) present in meningeal vessels, cardinal vein, and dorsal aorta. Moreover, small intersomitic vessels failed to form (Fig. 5B, lower panel), suggesting that deregulated PI3K activity results in lethal impairment of small vessel formation (*17*). These malformations were also evident in whole-mount embryo CD31 staining, with aberrant formation of the cephalic and intersomitic vessels (Fig. 5, C and D, upper panels). Morphology, proliferation, and apoptosis were not altered in *PIK3CA*$^{Tie2\text{-}Cre}$ embryos' hearts (fig. S7, B to D), suggesting that the observed phenotype is caused by a defect specifically affecting blood vessel formation. Aiming to validate the implication of excessive PI3K signaling in aberrant vasculogenesis, as well as to evaluate whether pharmacological inhibition could overcome this effect, we attempted to revert the phenotype by treating pregnant mice with the PI3Kα inhibitor BYL719. *PIK3CA*$^{Tie2\text{-}Cre}$ E9.5 embryos treated with the PI3Kα inhibitor showed an overall body size comparable to *PIK3CA*^{WT} littermates, suggesting improved vascular function (fig. S7E). CD31 whole-mount staining revealed restored cephalic and intersomitic small blood vessel formation (Fig. 5, C and D, lower panels). Phosphorylated AKT staining showed a strong reduction in both *PIK3CA*$^{Tie2\text{-}Cre}$ and *PIK3CA*^{WT} embryos after PI3Kα inhibitor treatment, in contrast with untreated control embryos (fig. S7F). At the histologic level, treatment reestablished meningeal, cardinal vein, and dorsal aorta blood vessel morphology (Fig. 5E), indicating that aberrant PI3K pathway hyperactivation impairs normal embryonic angiogenesis in mice.

DISCUSSION

VM are the most common vascular malformation in humans (*5*) and are a cause of pain, functional limitations of the affected areas, aesthetic disfigurements, and coagulopathies. In severe cases, sclerotherapy or surgical resection may be considered; however, these procedures often involve complications such as cutaneous necrosis or extended inflammatory reactions (*53*), and depending on the anatomic location and extension may have limited applicability. Moreover, VM are prone to recur and recanalize (*54*), raising the need for developing more effective therapies.

GEMMs represent reliable tools for investigating the etiology, biology, and progression of human diseases, as well as for exploring new therapeutic approaches (*55*, *56*). The first somatic molecular alterations linked to the development of sporadic VM were the acquisition of gain-of-function mutations in the gene encoding the EC-specific tyrosine kinase receptor TIE2 (*TEK*) (*6*, *8*, *57*, *58*). Ligand-independent receptor activation drives constitutive activation of the PI3K/AKT and MAPK pathways, resulting in increased proliferation and survival of EC that could account for increased EC accumulation in VM and abnormal recruitment of smooth muscle cells. However, only a subgroup of VM harbor defects in *TEK*, suggesting that other genomic or molecular alterations may be at play in this disease. In this line, it would be interesting to develop a GEMM expressing activating *TEK* mutations in the endothelial compartment to characterize in detail their role in the histopathology and the mechanism of pathogenesis of this disease.

Recent studies performing xenograft experiments with HUVECs transduced with the most frequent *TEK* mutation, L914F, have demonstrated its functional relevance in inducing VM (*11*). Treatment of murine xenografts with rapamycin proved the efficacy of inhibiting mTOR activity, which also showed clinical activity in VM patients in a pilot trial. Intriguingly, three of five patients that responded to mTOR inhibition in this study did not harbor any genetic defect in *TEK* (*11*). It is thus tempting to speculate that additional molecular alterations enhancing the activity of the PI3K/AKT/mTOR pathway could be driving the formation of VM in these patients.

We report the generation of a GEMM for VM by inducing the expression of the gain-of-function *PIK3CA*^{H1047R} mutant allele in mice. The histopathologic resemblance of the lesions arising in mice to those affecting humans prompted us to evaluate the existence of similar alterations in clinical specimens. Through targeted exome sequencing, we found that 25% of the evaluated samples bear activating mutations in *PIK3CA* or additional genetic defects predicted to stimulate constitutive downstream signaling. To reconcile our findings with those previously reported, we confirmed that 35% of the patients harbored mutations in *TEK*, yet these were mutually exclusive with the presence of activating PI3K mutations, consistent with a functional redundancy. These results are in agreement with the high prevalence of *TEK* mutations reported by others, mainly in pediatric patients (*6*, *7*).

TIE2 activated as a result of *TEK* mutations mainly signals through PI3K (*9*, *39*, *59*), consistent with the unifying hypothesis that aberrant activation of PI3K signaling by mutations in the upstream receptor or in the pathway itself causes the development of VM.

Somatic mutation of *PIK3CA* is frequently detected in several cancer types, and genetic alterations driving hyperactivation of the PI3K/AKT pathway have also been reported in nonhereditary postzygotic tissue overgrowth syndromes that often exhibit mixed capillary, lymphatic, and venous anomalies. Because of the clinical overlap of these overgrowth syndromes with *PIK3CA* mutations, the term *PIK3CA*-related overgrowth syndrome has been proposed (*19*). Patients suffering from congenital lipomatous overgrowth, vascular malformations, epidermal nevi, and skeletal/spinal abnormalities (CLOVES) syndrome harbor somatic mosaicism for activating *PIK3CA* mutations resulting in hyperactive PI3K/AKT signaling (*60*). The presence of somatic mutations in *PIK3CA* was also detected in patients affected by Klippel-Trenaunay-Weber syndrome, an overgrowth condition with features overlapping those of CLOVES syndrome: isolated lymphatic malformations, fibroadipose hyperplasia, and fibroadipose vascular anomalies (*61*, *62*). Additional genetic alterations in *PTEN*, *GNAQ*, AKT isoforms, or the regulatory subunit of PI3K *PIK3R1*, which enhance PI3K/AKT/mTOR and MAPK pathway activation, have also been reported in other malformation syndromes including Proteus (*63*), megalencephaly-capillary malformation (MCAP) (*64*), Sturge-Weber (*65*), and Bannayan-Riley-Ruvalcaba (*66*) syndromes, underscoring the involvement of aberrant PI3K/AKT/mTOR signaling in developmental disorders. The MCAP syndrome exhibits a predominant brain overgrowth phenotype in which *PIK3CA* mutations are also involved. A recent report has described the first mouse model for brain overgrowth using GEMM of *PIK3CA* mutants E545K and H1047R, validating the importance of these mouse models in the study of *PIK3CA*-driven syndromes (*67*). Nevertheless, sporadic and solitary VM lesions are a different and much more prevalent entity that is not necessarily associated with overgrowth.

Despite the fact that most lymphatic malformations carry *PIK3CA* mutations, our mouse model does not present detectable lymphatic anomalies. This is a limitation of our model that could be explained by a number of factors including the moment and time of recombination, or possibly different sets of precursor cells giving rise to each malformation. Our observations are further supported by those made by Castillo and colleagues, who found that mosaic somatic mutations induced in a $PIK3CA^{H1047R}$ mouse model cause VM that are associated with neither tissue overgrowth nor lymphatic malformations (*45*), suggesting that the cell of origin giving rise to VM may be more susceptible to hyperactive PI3K signaling than other cell lineages and that additional genetic or environmental cues are required to reproduce the complex phenotypes observed in overgrowth syndromes. In the future, it would also be interesting to identify the cell of origin of VM by means of lineage-tracing experiments.

Given the ability of our mouse model to recapitulate the pathogenesis of human VM, we determined whether it could be used as a platform for testing pharmacological inhibition using PI3K inhibitors currently under clinical development. To put it into context, we also evaluated the efficacy of other agents that have been proposed to inhibit the growth of VM, including rapamycin analogs and propranolol (*11*, *68*). The greatest growth inhibition was achieved when treating allograft transplants with a PI3Kα inhibitor or the rapamycin analog everolimus, but no effect was observed with propranolol. Rapamycin improves quality of life in patients with VM (*11*), lymphatic malformations (*69*), and other vascular syndromes (*48*),

probably because long-term treatment with rapamycin has the ability to inhibit AKT in ECs; this observation is also seen in adipocytes, but not in all epithelial cells (*70*).

In contrast to the antiproliferative effect of rapamycin analogs, we propose that the proapoptotic effect achieved upon PI3K inhibition is likely to yield improved therapeutic efficacy by diminishing the recurrence of VM. Topical administration of PI3Kα inhibitor further demonstrated the efficacy of this treatment with an approach that would be devoid of the substantial side effects associated with systemic drug administration (hyperglycemia, nausea, gastrointestinal effects, and fatigue) (*50*). The impaired vasculogenesis observed in mouse embryos as a consequence of endothelial-restricted expression of the *PIK3CA*^{H1047R} allele was also rescued when pregnant mice were treated with the PI3Kα inhibitor, further supporting a functional requirement for controlled PI3K signaling in normal embryonic vasculogenesis as has been demonstrated by others (*51*).

In summary, our study provides a GEMM recapitulating human VM caused by hyperactivation of the PI3K/AKT pathway, reveals the impact of *PIK3CA* somatic mutations in the pathogenesis of VM, and provides a potential therapeutic approach to treat advanced or recurrent lesions in these patients.

MATERIALS AND METHODS

Materials and methods can be found in the Supplementary Materials.

Supplementary Material

Refer to Web version on PubMed Central for supplementary material.

Acknowledgments

We thank P. Zanzonico and V. Longo from the Animal Imaging Core; M. Turkekul, V. Boyko, and D. Yarilin from the Molecular Cytology Core; and G. Nanjangud from the Molecular Cytogenetics Core. We also thank M. Lepherd from the Laboratory of Comparative Pathology. We thank the MSKCC (Memorial Sloan Kettering Cancer Center) Center for Molecular Oncology, the Integrated Genomics Operation, K. Huberman, and N. Socci for the assistance with DNA sequencing and data analysis. We thank J. Bischoff and M. Valiente for providing cell lines and G. Minuesa for help with flow cytometry. **Funding:** Supported by Geoffrey Beene Cancer Center. The Molecular Cytology Core is supported by grant P30 CA008748J. The Integrated Genomics Operation is supported by grant P30 CA008748. J.G.-B. is supported by the Secretary for Universities and Research of the Government of Catalonia and the COFUND program of the Marie Curie Actions of the 7th R&D Framework Programme of the European Union. F.J.C. holds a fellowship from the Terri Brodeur Breast Cancer Foundation. K.V.A. was funded by NIH R01 NS 044385.

REFERENCES AND NOTES

1. Brouillard P, Vikkula M. Genetic causes of vascular malformations. Hum. Mol. Gen. 2007; 16:R140–R149. [PubMed: 17670762]
2. Brouillard P, Vikkula M. Vascular malformations: Localized defects in vascular morphogenesis. Clin. Genet. 2003; 63:340–351. [PubMed: 12752563]
3. Dompmartin A, Vikkula M, Boon LM. Venous malformation: Update on aetiopathogenesis, diagnosis and management. Phlebology. 2010; 25:224–235. [PubMed: 20870869]
4. Nguyen H-L, Boon LM, Vikkula M. Genetics of vascular malformations. Semin. Pediatr. Surg. 2014; 23:221–226. [PubMed: 25241102]

5. Uebelhoer M, Boon LM, Vikkula M. Vascular anomalies: From genetics toward models for therapeutic trials. Cold Spring Harb. Perspect. Med. 2012; 2:a009688. [PubMed: 22908197]
6. Limaye N, Wouters V, Uebelhoer M, Tuominen M, Wirkkala R, Mulliken JB, Eklund L, Boon LM, Vikkula M. Somatic mutations in angiopoietin receptor gene *TEK* cause solitary and multiple sporadic venous malformations. Nat. Genet. 2009; 41:118–124. [PubMed: 19079259]
7. Soblet J, Limaye N, Uebelhoer M, Boon LM, Vikkula M. Variable somatic *TIE2* mutations in half of sporadic venous malformations. Mol. Syndromol. 2013; 4:179–183. [PubMed: 23801934]
8. Vikkula M, Boon LM, Carraway KL III, Calvert JT, Diamonti AJ, Goumnerov B, Pasyk KA, Marchuk DA, Warman ML, Cantley LC, Mulliken JB, Olsen BR. Vascular dysmorphogenesis caused by an activating mutation in the receptor tyrosine kinase TIE2. Cell. 1996; 87:1181–1190. [PubMed: 8980225]
9. Kontos CD, Stauffer TP, Yang W-P, York JD, Huang L, Blanar MA, Meyer T, Peters KG. Tyrosine 1101 of Tie2 is the major site of association of p85 and is required for activation of phosphatidylinositol 3-kinase and Akt. Mol. Cell. Biol. 1998; 18:4131–4140. [PubMed: 9632797]
10. Morris PN, Dunmore BJ, Tadros A, Marchuk DA, Darland DC, D'Amore PA, Brindle NPJ. Functional analysis of a mutant form of the receptor tyrosine kinase Tie2 causing venous malformations. J. Mol. Med. 2005; 83:58–63. [PubMed: 15526080]
11. Boscolo E, Limaye N, Huang L, Kang K-T, Soblet J, Uebelhoer M, Mendola A, Natynki M, Seront E, Dupont S, Hammer J, Legrand C, Brugnara C, Eklund L, Vikkula M, Bischoff J, Boon LM. Rapamycin improves *TIE2*-mutated venous malformation in murine model and human subjects. J. Clin. Invest. 2015; 125:3491–3504. [PubMed: 26258417]
12. Uebelhoer M, Nätynki M, Kangas J, Mendola A, Nguyen H-L, Soblet J, Godfraind C, Boon LM, Eklund L, Limaye N, Vikkula M. Venous malformation-causative *TIE2* mutations mediate an AKT-dependent decrease in PDGFB. Hum. Mol. Genet. 2013; 22:3438–3448. [PubMed: 23633549]
13. Nätynki M, Kangas J, Miinalainen I, Sormunen R, Pietilä R, Soblet J, Boon LM, Vikkula M, Limaye N, Eklund L. Common and specific effects of *TIE2* mutations causing venous malformations. Hum. Mol. Genet. 2015; 24:6374–6389. [PubMed: 26319232]
14. Fruman DA, Rommel C. PI3K and cancer: Lessons, challenges and opportunities. Nat. Rev. Drug Discov. 2014; 13:140–156. [PubMed: 24481312]
15. Engelman JA. Targeting PI3K signalling in cancer: Opportunities, challenges and limitations. Nat. Rev. Cancer. 2009; 9:550–562. [PubMed: 19629070]
16. Keppler-Noreuil KM, Rios JJ, Parker VER, Semple RK, Lindhurst MJ, Sapp JC, Alomari A, Ezaki M, Dobyns W, Biesecker LG. PIK3CA-related overgrowth spectrum (PROS): Diagnostic and testing eligibility criteria, differential diagnosis, and evaluation. Am. J. Med. Genet. A. 2015; 167A:287–295. [PubMed: 25557259]
17. Graupera M, Guillermet-Guibert J, Foukas LC, Phng L-K, Cain RJ, Salpekar A, Pearce W, Meek S, Millan J, Cutillas PR, Smith AJH, Ridley AJ, Ruhrberg C, Gerhardt H, Vanhaesebroeck B. Angiogenesis selectively requires the p110a isoform of PI3K to control endothelial cell migration. Nature. 2008; 453:662–666. [PubMed: 18449193]
18. Graupera M, Potente M. Regulation of angiogenesis by PI3K signaling networks. Exp. Cell Res. 2013; 319:1348–1355. [PubMed: 23500680]
19. Kang H-C, Baek ST, Song S, Gleeson JG. Clinical and genetic aspects of the segmental overgrowth spectrum due to somatic mutations in *PIK3CA*. J. Pediatr. 2015; 167:957–962. [PubMed: 26340871]
20. Osborn AJ, Dickie P, Neilson DE, Glaser K, Lynch KA, Gupta A, Dickie BH. Activating PIK3CA alleles and lymphangiogenic phenotype of lymphatic endothelial cells isolated from lymphatic malformations. Hum. Mol. Genet. 2015; 24:926–938. [PubMed: 25292196]
21. Cancer Genome Atlas Research Network. Kandoth C, Schultz N, Cherniack AD, Akbani R, Liu Y, Shen H, Robertson AG, Pashtan I, Shen R, Benz CC, Yau C, Laird PW, Ding L, Zhang W, Mills GB, Kucherlapati R, Mardis ER, Levine DA. Integrated genomic characterization of endometrial carcinoma. Nature. 2013; 497:67–73. [PubMed: 23636398]

22. Adams JR, Xu K, Liu JC, Agamez NMR, Loch AJ, Wong RG, Wang W, Wright KL, Lane TF, Zacksenhaus E, Egan SE. Cooperation between PIK3CA and p53 mutations in mouse mammary tumor formation. Cancer Res. 2011; 71:2706–2717. [PubMed: 21324922]

23. Contreras CM, Akbay EA, Gallardo TD, Haynie JM, Sharma S, Tagao O, Bardeesy N, Takahashi M, Settleman J, Wong KK, Castrillon DH. Lkb1 inactivation is sufficient to drive endometrial cancers that are aggressive yet highly responsive to mTOR inhibitor monotherapy. Dis. Model. Mech. 2010; 3:181–193. [PubMed: 20142330]

24. Krings T. Vascular malformations of the spine and spinal cord*: Anatomy, classification, treatment. Clin. Neuroradiol. 2010; 20:5–24. [PubMed: 20229203]

25. Wassef M, Blei F, Adams D, Alomari A, Baselga E, Berenstein A, Burrows P, Frieden IJ, Garzon MC, Lopez-Gutierrez JC, Lord DJ, Mitchel S, Powell J, Prendiville J, Vikkula M, ISSVA Board and Scientific Committee. Vascular anomalies classification: Recommendations from the International Society for the Study of Vascular Anomalies. Pediatrics. 2015; 136:e203–e214. [PubMed: 26055853]

26. North PE, Waner M, Mizeracki A, Mihm MC Jr. GLUT1: A newly discovered immunohistochemical marker for juvenile hemangiomas. Hum. Pathol. 2000; 31:11–22. [PubMed: 10665907]

27. Lawley LP, Cerimele F, Weiss SW, North P, Cohen C, Kozakewich HPW, Mulliken JB, Arbiser JL. Expression of Wilms tumor 1 gene distinguishes vascular malformations from proliferative endothelial lesions. Arch. Dermatol. 2005; 141:1297–1300. [PubMed: 16230568]

28. Léauté-Labrèze C, Hoeger P, Mazereeuw-Hautier J, Guibaud L, Baselga E, Posiunas G, Phillips RJ, Caceres H, Lopez Gutierrez JC, Ballona R, Friedlander SF, Powell J, Perek D, Metz B, Barbarot S, Maruani A, Szalai ZZ, Krol A, Boccara O, Foelster-Holst R, Febrer Bosch MI, Su J, Buckova H, Torrelo A, Cambazard F, Grantzow R, Wargon O, Wyrzykowski D, Roessler J, Bernabeu-Wittel J, Valencia AM, Przewratil P, Glick S, Pope E, Birchall N, Benjamin L, Mancini AJ, Vabres P, Souteyrand P, Frieden IJ, Berul CI, Mehta CR, Prey S, Boralevi F, Morgan CC, Heritier S, Delarue A, Voisard J-J. A randomized, controlled trial of oral propranolol in infantile hemangioma. N. Engl. J. Med. 2015; 372:735–746. [PubMed: 25693013]

29. Brouillard P, Boon L, Vikkula M. Genetics of lymphatic anomalies. J. Clin. Invest. 2014; 124:898–904. [PubMed: 24590274]

30. Mouta-Bellum C, Kirov A, Miceli-Libby L, Mancini ML, Petrova TV, Liaw L, Prudovsky I, Thorpe PE, Miura N, Cantley LC, Alitalo K, Fruman DA, Vary CPH. Organ-specific lymphangiectasia, arrested lymphatic sprouting, and maturation defects resulting from gene-targeting of the PI3K regulatory isoforms p85α, p55α, and p50α. Dev. Dyn. 2009; 238:2670–2679. [PubMed: 19705443]

31. Banerji S, Ni J, Wang SX, Clasper S, Su J, Tammi R, Jones M, Jackson DG. LYVE-1, a new homologue of the CD44 glycoprotein, is a lymph-specific receptor for hyaluronan. J. Cell Biol. 1999; 144:789–801. [PubMed: 10037799]

32. Castro EC, Galambos C. Prox-1 and VEGFR3 antibodies are superior to D2–40 in identifying endothelial cells of lymphatic malformations—A proposal of a new immunohistochemical panel to differentiate lymphatic from other vascular malformations. Pediatr. Dev. Pathol. 2009; 12:187–194. [PubMed: 18937526]

33. Arnaoutova I, George J, Kleinman HK, Benton G. The endothelial cell tube formation assay on basement membrane turns 20: State of the science and the art. Angiogenesis. 2009; 12:267–274. [PubMed: 19399631]

34. Tian XL, Kadaba R, You SA, Liu M, Timur AA, Yang L, Chen Q, Szafranski P, Rao S, Wu L, Housman DE, DiCorleto PE, Driscoll DJ, Borrow J, Wang Q. Identification of an angiogenic factor that when mutated causes susceptibility to Klippel–Trenaunay syndrome. Nature. 2004; 427:640–645. [PubMed: 14961121]

35. Daly C, Pasnikowski E, Burova E, Wong V, Aldrich TH, Griffiths J, Ioffe E, Daly TJ, Fandl JP, Papadopoulos N, McDonald DM, Thurston G, Yancopoulos GD, Rudge JS. Angiopoietin-2 functions as an autocrine protective factor in stressed endothelial cells. Proc. Natl. Acad. Sci. U.S.A. 2006; 103:15491–15496. [PubMed: 17030814]

36. Thurston G, Daly C. The complex role of angiopoietin-2 in the angiopoietin–tie signaling pathway. Cold Spring Harb. Perspect. Med. 2012; 2:a006550. [PubMed: 22951441]

37. Cheng DT, Mitchell TN, Zehir A, Shah RH, Benayed R, Syed A, Chandramohan R, Liu ZY, Won HH, Scott SN, Brannon AR, O'Reilly C, Sadowska J, Casanova J, Yannes A, Hechtman JF, Yao J, Song W, Ross DS, Oultache A, Dogan S, Borsu L, Hameed M, Nafa K, Arcila ME, Ladanyi M, Berger MF. Memorial Sloan Kettering-Integrated Mutation Profiling of Actionable Cancer Targets (MSK-IMPACT): A hybridization capture-based next-generation sequencing clinical assay for solid tumor molecular oncology. J. Mol. Diagn. 2015; 17:251–264. [PubMed: 25801821]
38. Samuels Y, Diaz LA Jr. Schmidt-Kittler O, Cummins JM, Delong L, Cheong I, Rago C, Huso DL, Lengauer C, Kinzler KW, Vogelstein B, Velculescu VE. Mutant PIK3CA promotes cell growth and invasion of human cancer cells. Cancer Cell. 2005; 7:561–573. [PubMed: 15950905]
39. Jones N, Master Z, Jones J, Bouchard D, Gunji Y, Sasaki H, Daly R, Alitalo K, Dumont DJ. Identification of *TEK/Tie2* binding partners. Binding to a multifunctional docking site mediates cell survival and migration. J. Biol. Chem. 1999; 274:30896–30905. [PubMed: 10521483]
40. Hayashi S, McMahon AP. Efficient recombination in diverse tissues by a tamoxifen-inducible form of Cre: A tool for temporally regulated gene activation/inactivation in the mouse. Dev. Biol. 2002; 244:305–318. [PubMed: 11944939]
41. Ruzankina Y, Pinzon-Guzman C, Asare A, Ong T, Pontano L, Cotsarelis G, Zediak VP, Velez M, Bhandoola A, Brown EJ. Deletion of the developmentally essential gene *ATR* in adult mice leads to age-related phenotypes and stem cell loss. Cell Stem Cell. 2007; 1:113–126. [PubMed: 18371340]
42. Adams RH, Alitalo K. Molecular regulation of angiogenesis and lymphangiogenesis. Nat. Rev. Mol. Cell Biol. 2007; 8:464–478. [PubMed: 17522591]
43. Smith MC, Li DY, Whitehead KJ. Mechanisms of vascular stability and the relationship to human disease. Curr. Opin. Hematol. 2010; 17:237–244. [PubMed: 20308891]
44. Herbert SP, Stainier DYR. Molecular control of endothelial cell behaviour during blood vessel morphogenesis. Nat. Rev. Mol. Cell Biol. 2011; 12:551–564. [PubMed: 21860391]
45. Castillo SD, Tzouanacou E, Zaw-Thin M, Berenjeno IM, Parker V, Chivite I, Milà-Guasch M, Pearce W, Solomon I, Angulo-Urarte A, Figueiredo AM, Dewhurst RE, Knox RG, Clark GR, Scudamore CL, Badar A, Kalber TL, Foster J, Stuckey DJ, David AL, Phillips WA, Lythgoe MF, Wilson V, Semple RK, Sebire NJ, Kinsler VA, Graupera M, Vanhaesebroeck B. Somatic activating mutations in *Pik3ca* cause sporadic venous malformations in mice and humans. Sci. Transl. Med. 2016; 8:332ra43.
46. Dompmartin A, Ballieux F, Thibon P, Lequerrec A, Hermans C, Clapuyt P, Barrellier M-T, Hammer F, Labbé D, Vikkula M, Boon LM. Elevated D-dimer level in the differential diagnosis of venous malformations. Arch. Dermatol. 2009; 145:1239–1244. [PubMed: 19917952]
47. Fritsch C, Huang A, Chatenay-Rivauday C, Schnell C, Reddy A, Liu M, Kauffmann A, Guthy D, Erdmann D, De Pover A, Furet P, Gao H, Ferretti S, Wang Y, Trappe J, Brachmann SM, Maira S-M, Wilson C, Boehm M, Garcia-Echeverria C, Chene P, Wiesmann M, Cozens R, Lehar J, Schlegel R, Caravatti G, Hofmann F, Sellers WR. Characterization of the novel and specific PI3Kα inhibitor NVP-BYL719 and development of the patient stratification strategy for clinical trials. Mol. Cancer Ther. 2014; 13:1117–1129. [PubMed: 24608574]
48. Lackner H, Karastaneva A, Schwinger W, Benesch M, Sovinz P, Seidel M, Sperl D, Lanz S, Haxhija E, Reiterer F, Sorantin E, Urban CE. Sirolimus for the treatment of children with various complicated vascular anomalies. Eur. J. Pediatr. 2015; 174:1579–1584. [PubMed: 26040705]
49. Hammill AM, Wentzel M, Gupta A, Nelson S, Lucky A, Elluru R, Dasgupta R, Azizkhan RG, Adams DM. Sirolimus for the treatment of complicated vascular anomalies in children. Pediatr. Blood Cancer. 2011; 57:1018–1024. [PubMed: 21445948]
50. Rodon J, Dienstmann R, Serra V, Tabernero J. Development of PI3K inhibitors: Lessons learned from early clinical trials. Nat. Rev. Clin. Oncol. 2013; 10:143–153. [PubMed: 23400000]
51. Hare LM, Schwarz Q, Wiszniak S, Gurung R, Montgomery KG, Mitchell CA, Phillips WA. Heterozygous expression of the oncogenic PIK3CA(H1047R) mutation during murine development results in fatal embryonic and extraembryonic defects. Dev. Biol. 2015; 404:14–26. [PubMed: 25958091]
52. Kisanuki YY, Hammer RE, Miyazaki J.-i. Williams SC, Richardson JA, Yanagisawa M. Tie2-Cre transgenic mice: A new model for endothelial cell-lineage analysis in vivo. Dev. Biol. 2001; 230:230–242. [PubMed: 11161575]

53. Cox JA, Bartlett E, Lee EI. Vascular Malformations: A review. Semin. Plast. Surg. 2014; 28:58–63. [PubMed: 25045330]
54. de Lorimier AA. Sclerotherapy for venous malformations. J. Pediatr. Surg. 1995; 30:188–194. [PubMed: 7738736]
55. Heyer J, Kwong LN, Lowe SW, Chin L. Non-germline genetically engineered mouse models for translational cancer research. Nat. Rev. Cancer. 2010; 10:470–480. [PubMed: 20574449]
56. van Miltenburg MH, Jonkers J. Using genetically engineered mouse models to validate candidate cancer genes and test new therapeutic approaches. Curr. Opin. Genet. Dev. 2012; 22:21–27. [PubMed: 22321988]
57. Calvert JT, Riney TJ, Kontos CD, Cha EH, Prieto VG, Shea CR, Berg JN, Nevin NC, Simpson SA, Pasyk KA, Speer MC, Peters KG, Marchuk DA. Allelic and locus heterogeneity in inherited venous malformations. Hum. Mol. Genet. 1999; 8:1279–1289. [PubMed: 10369874]
58. Wouters V, Limaye N, Uebelhoer M, Irrthum A, Boon LM, Mulliken JB, Enjolras O, Baselga E, Berg J, Dompmartin A, Ivarsson SA, Kangesu L, Lacassie Y, Murphy J, Teebi AS, Penington A, Rieu P, Vikkula M. Hereditary cutaneomucosal venous malformations are caused by TIE2 mutations with widely variable hyper-phosphorylating effects. Eur. J. Hum. Genet. 2010; 18:414–420. [PubMed: 19888299]
59. Kim I, Kim HG, So J-N, Kim JH, Kwak HJ, Koh GY. Angiopoietin-1 regulates endothelial cell survival through the phosphatidylinositol 3′-kinase/Akt signal transduction pathway. Circ. Res. 2000; 86:24–29. [PubMed: 10625301]
60. Kurek KC, Luks VL, Ayturk UM, Alomari AI, Fishman SJ, Spencer SA, Mulliken JB, Bowen ME, Yamamoto GL, Kozakewich HP, Warman ML. Somatic mosaic activating mutations in *PIK3CA* cause CLOVES syndrome. Am. J. Hum. Genet. 2012; 90:1108–1115. [PubMed: 22658544]
61. Luks VL, Kamitaki N, Vivero MP, Uller W, Rab R, Bovée JVMG, Rialon KL, Guevara CJ, Alomari AI, Greene AK, Fishman SJ, Kozakewich HPW, Maclellan RA, Mulliken JB, Rahbar R, Spencer SA, Trenor CC III, Upton J, Zurakowski D, Perkins JA, Kirsh A, Bennett JT, Dobyns WB, Kurek KC, Warman ML, McCarroll SA, Murillo R. Lymphatic and other vascular malformative/overgrowth disorders are caused by somatic mutations in *PIK3CA*. J. Pediatr. 2015; 166:1048–1054. [PubMed: 25681199]
62. Lindhurst MJ, Parker VER, Payne F, Sapp JC, Rudge S, Harris J, Witkowski AM, Zhang Q, Groeneveld MP, Scott CE, Daly A, Huson SM, Tosi LL, Cunningham ML, Darling TN, Geer J, Gucev Z, Sutton VR, Tziotzios C, Dixon AK, Helliwell T, O'Rahilly S, Savage DB, Wakelam MJO, Barroso I, Biesecker LG, Semple RK. Mosaic overgrowth with fibroadipose hyperplasia is caused by somatic activating mutations in *PIK3CA*. Nat. Genet. 2012; 44:928–933. [PubMed: 22729222]
63. Lindhurst MJ, Sapp JC, Teer JK, Johnston JJ, Finn EM, Peters K, Turner J, Cannons JL, Bick D, Blakemore L, Blumhorst C, Brockmann K, Calder P, Cherman N, Deardorff MA, Everman DB, Golas G, Greenstein RM, Kato BM, Keppler-Noreuil KM, Kuznetsov SA, Miyamoto RT, Newman K, Ng D, O'Brien K, Rothenberg S, Schwartzentruber DJ, Singhal V, Tirabosco R, Upton J, Wientroub S, Zackai EH, Hoag K, Whitewood-Neal T, Robey PG, Schwartzberg PL, Darling TN, Tosi LL, Mullikin JC, Biesecker LG. A mosaic activating mutation in *AKT1* associated with the Proteus syndrome. N. Engl. J. Med. 2011; 365:611–619. [PubMed: 21793738]
64. Rivière J-B, Mirzaa GM, O'Roak BJ, Beddaoui M, Alcantara D, Conway RL, St-Onge J, Schwartzentruber JA, Gripp KW, Nikkel SM, Worthylake T, Sullivan CT, Ward TR, Butler HE, Kramer NA, Albrecht B, Armour CM, Armstrong L, Caluseriu O, Cytrynbaum C, Drolet BA, Innes AM, Lauzon JL, Lin AE, Mancini GMS, Meschino WS, Reggin JD, Saggar AK, Lerman-Sagie T, Uyanik G, Weksberg R, Zirn B, Beaulieu CL, Finding of Rare Disease Genes (FORGE) Canada Consortium. Majewski J, Bulman DE, O'Driscoll M, Shendure J, Graham JM Jr. Boycott KM, Dobyns WB. De novo germline and postzygotic mutations in *AKT3*, *PIK3R2* and *PIK3CA* cause a spectrum of related megalencephaly syndromes. Nat. Genet. 2012; 44:934–940. [PubMed: 22729224]
65. Shirley MD, Tang H, Gallione CJ, Baugher JD, Frelin LP, Cohen B, North PE, Marchuk DA, Comi AM, Pevsner J. Sturge–Weber syndrome and port-wine stains caused by somatic mutation in *GNAQ*. N. Engl. J. Med. 2013; 368:1971–1979. [PubMed: 23656586]

66. Marsh DJ, Dahia PLM, Zheng Z, Liaw D, Parsons R, Gorlin RJ, Eng C. Germline mutations in *PTEN* are present in Bannayan-Zonana syndrome. Nat. Genet. 1997; 16:333–334. [PubMed: 9241266]

67. Roy A, Ni J, Skibo J, Rankin S, Dobyns WB, Kalume F, Baker SJ, Zhao J, Millen KJ. Modeling human PIK3CA-related congenital brain overgrowth and epilepsy in mice. Int. J. Dev. Neurosci. 2015; 47:46.

68. Pföhler C, Janssen E, Buecker A, Vogt T, Müller CSL. Successful treatment of a congenital extra-truncal vascular malformation by orally administered propranolol. J. Dermatol. Treat. 2015; 26:59–62.

69. Blatt J, McLean TW, Castellino SM, Burkhart CN. A review of contemporary options for medical management of hemangiomas, other vascular tumors, and vascular malformations. Pharmacol. Ther. 2013; 139:327–333. [PubMed: 23665062]

70. Sarbassov DD, Ali SM, Sengupta S, Sheen J-H, Hsu PP, Bagley AF, Markhard AL, Sabatini DM. Prolonged rapamycin treatment inhibits mTORC2 assembly and Akt/PKB. Mol. Cell. 2006; 22:159–168. [PubMed: 16603397]

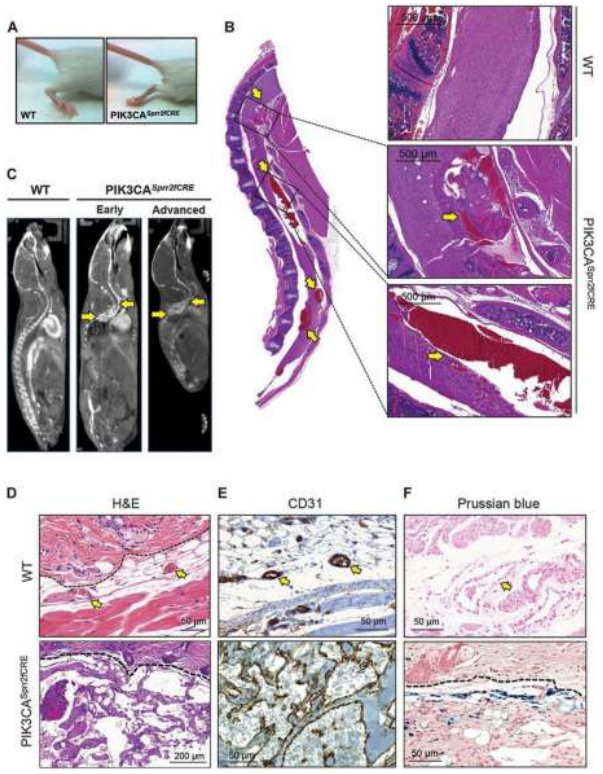

Fig. 1. *PIK3CA*$^{\text{Sprr2fCRE}}$ mice develop spinal vascular malformations

(**A**) Hindlimb paresis phenotype observed in *PIK3CA*$^{\text{Sprr2fCRE}}$ mice. WT, wild type. (**B**) Gross and detailed histology of the spinal cord of *PIK3CA*$^{\text{Sprr2fCRE}}$ mice compared to a normal WT spine. Arrows indicate the multiple focal hemorrhages found in the spinal cord. (**C**) microCT (micro-computed tomography) scan of a WT mouse compared to *PIK3CA*$^{\text{Sprr2fCRE}}$ mice littermates showing an early and an advanced phenotype. Arrows indicate the slow flow and extravasation lesions observed in the spinal cord. (**D**) Hematoxylin and eosin (H&E) histology from normal skin and cutaneous VM. Dashed line delimits the dermis (lower) from the epidermis (upper). Arrows indicate normal blood vessels. (**E**) CD31 immunohistochemistry (IHC) of the skin VM lesions. Arrows indicate normal blood vessels. (**F**) Prussian blue staining. Dashed line delimits the dermis (lower) from the epidermis (upper). Arrow indicates normal blood vessel.

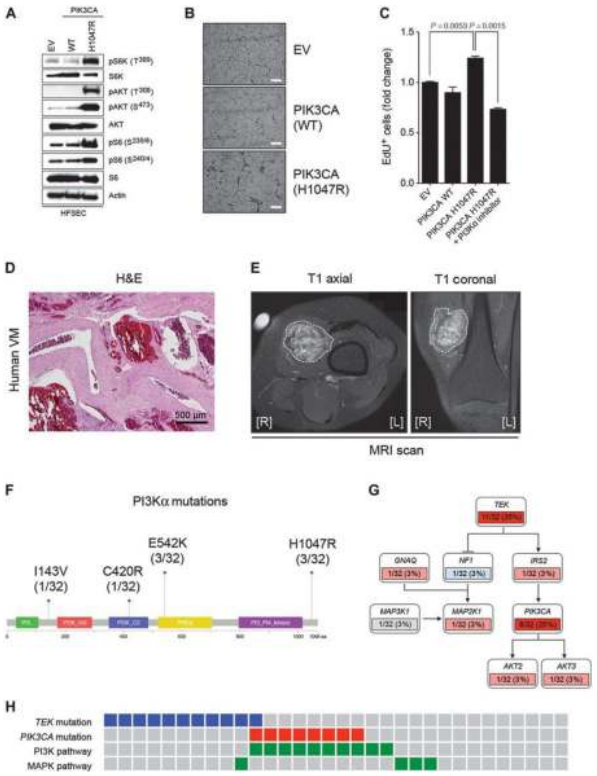

Fig. 2. *PIK3CA* mutations cause sporadic VM in humans

(**A**) Western blot of human skin ECs infected with empty vector (EV), *PIK3CA* WT, and H1047R mutation probed with the indicated antibodies. Cells were serum-starved overnight before lysis. S6K, S6 kinase; pS6K, phosphorylated S6K; pS6, phosphorylated S6; pAKT, phospshorylated AKT; HFSEC, human female skin endothelial cell. (**B**) Representative images from the tube formation assays of primary ECs infected with EV, *PIK3CA* WT, and H1047R mutation and serum-starved overnight before seeding. Pictures were taken 6 hours after seeding. Note the reticular network formed in the EV and PIK3CA WT cells that fails to form in the PIK3CA H1047R mutant cells. Scale bars, 200 μm. (**C**) EdU incorporation assay quantification of ECs infected with EV, *PIK3CA* WT, and H1047R mutation, serum-starved overnight, and labeled with EdU for 4 hours. Graph shows mean fold change ± SEM. $n = 3$ biological replicates. P values were calculated using Student's t test. (**D**) H&E staining highlighting the representative morphology of one of the human VM patients sequenced in this study. Blood pools and thick mural cell layer are evident in the histological sections of these patients. (**E**) Characteristic MRI scan from an intramuscular sporadic VM patient sequenced in this study. T1 axial and coronal sections are shown. Dashed line delimits the radiological extension of the malformation. [R] and [L] indicate right and left, respectively. (**F**) PI3Kα domains and specific sites found to be mutated in this study. The p85-binding domain is represented in green, the Rasbinding domain in red, the C2 domain in blue, the helical domain in yellow, and the kinase domain in purple. aa, amino acid. (**G**) Schematic pathway depicting TIE2, PI3K, and MAPK pathway gene components found to be mutated in sporadic VM by MSK-IMPACT in this study. Activating mutations are indicated in red and inactivating mutations in blue. Dark red designates mutations found in more than 20% of the patients. Unknown mutations are shown in gray. (**H**) Mutual

exclusivity of the gene mutations present in the *TEK* and *PIK3CA* pathways. The activating mutations in *TEK* are indicated in blue, and the activating mutations in *PIK3CA* are in red. The alterations affecting genes involved in the PI3K or MAPK pathway are represented in green.

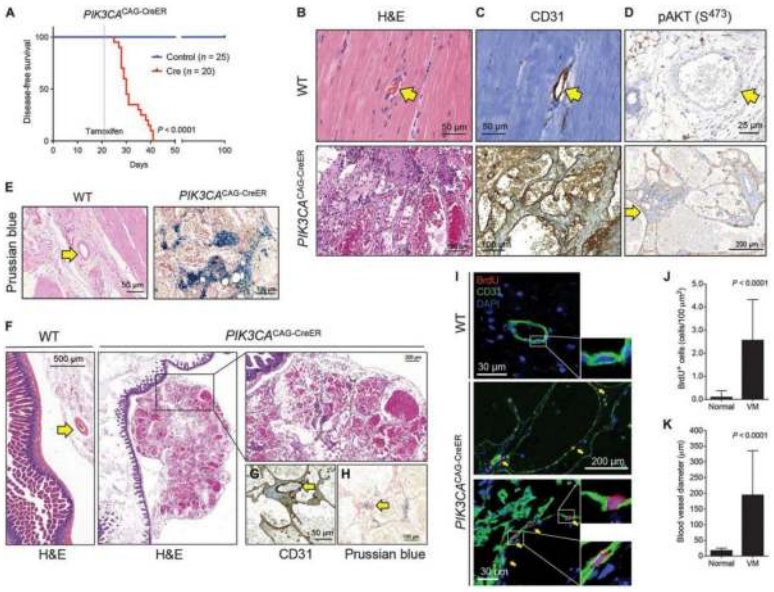

Fig. 3. Ubiquitous expression of *PIK3CA*^{H1047R} induces VM

(**A**) Disease-free survival plot of *PIK3CA*$^{CAG\text{-}CreER}$ ($n = 20$) and *PIK3CA*^{WT} ($n = 25$) littermates on tamoxifen diet assessed by the appearance of visible cutaneous VM. Dotted line represents the time when tamoxifen diet was administered (day 21). *P* value was calculated using log-rank test. (**B**) H&E staining of a representative normal blood vessel and a VM lesion developed in the skin of *PIK3CA*$^{CAG\text{-}CreER}$ mice. Arrow indicates normal blood vessel. (**C**) CD31 IHC staining showing positivity for the ECs of a normal blood vessel and VM. Note that erythrocytes exhibit nonspecific staining. Arrow indicates normal blood vessel. (**D**) Phosphorylated AKT (S^{473}) IHC. The arrow in the bottom panel indicates lining ECs that show positivity for the staining. Note the negativity for phosphorylated AKT in the normal blood vessel (top, indicated by an arrow). (**E**) Prussian blue staining of normal blood vessels and the *PIK3CA*$^{CAG\text{-}CreER}$ mouse skin VM lesions. Arrow indicates a normal blood vessel. (**F**) Histological representation of mesenteric vasculature and VM harvested during necropsy and detailed view to highlight the blood pools observed in the preparations. Arrows indicate normal blood vessels. (**G** and **H**) CD31 (G) and Prussian blue (H) positivity for the VM described in (F). (**I**) BrdU incorporation (red) in *PIK3CA*$^{CAG\text{-}CreER}$ VM compared to normal blood vessels. CD31 (green) and DAPI (4′,6-diamidino-2-phenylindole) (blue) show ECs and nuclei, respectively. Note the encased BrdU-positive nuclei in the CD31-positive lining EC layer. (**J**) Quantification of BrdU-positive nuclei in normal blood vessels and VM. *P* value was calculated using Student's *t* test. Graph shows means ± SD. $n = 45$ fields from five biological replicates. (**K**) Morphological quantification of the maximal blood vessel diameter of normal vessels and VM. *P* value was calculated using Student's *t* test. Graph shows means ± SD. $n = 45$ fields from five biological replicates.

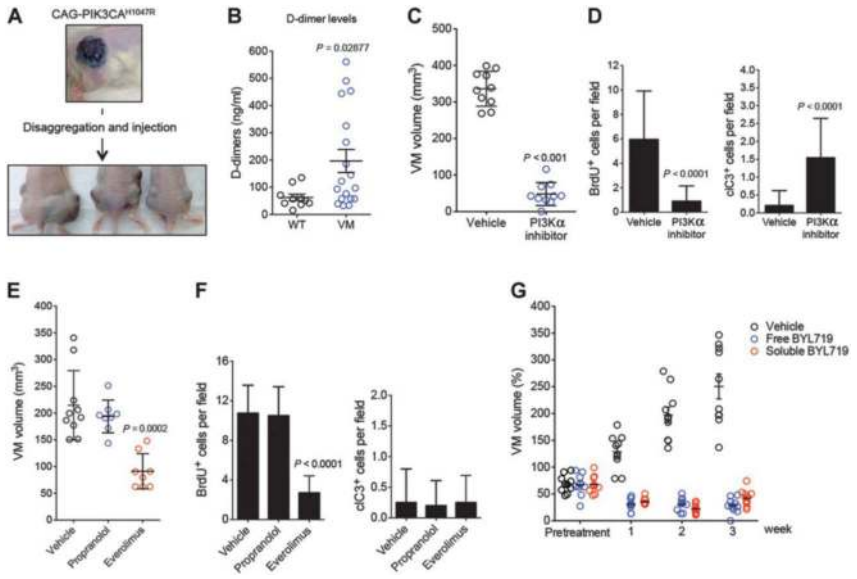

Fig. 4. PI3K inhibitors are effective for the treatment of VM

(**A**) Schematic representation and images from the allotransplantation assays. (**B**) Quantification of plasma D-dimers measured in animals with or without VM. *P* value was calculated using Student's *t* test. (**C**) VM volume measured in *PIK3CA*$^{\text{CAG-CreER}}$ VM-derived allografts treated with vehicle or PI3Kα inhibitor for 1 week [BYL719, 50 mg kg^{-1}, daily, per os (po)]. *P* value was calculated using Student's *t* test. (**D**) Quantification of BrdU incorporation and cleaved caspase-3 (clC3) in CD31-positive cells from (B). *P* value was calculated using Student's *t* test. $n = 10$. (**E**) VM volume measured in *PIK3CA*$^{\text{CAG-CreER}}$ VM-derived allografts treated with vehicle, everolimus (10 mg kg^{-1}, daily, po), or propranolol (40 mg kg^{-1}, daily, po) for 1 week. *P* value was calculated using Student's *t* test. (**F**) Quantification of BrdU incorporation and cleaved caspase-3 in CD31-positive cells from (E). *P* value was calculated using Student's *t* test. $n = 8$. (**G**) VM volume in *PIK3CA*$^{\text{CAG-CreER}}$ VM-derived allografts treated topically with BYL719 at 1% (w/w) using two different formulations (free and soluble BYL719) for 3 weeks. The pretreatment time point indicates when the treatment was started. All treatments in weeks 1, 2, and 3 have a $P < 0.001$ as compared to the vehicle control VM. *P* values were calculated using Student's *t* test.

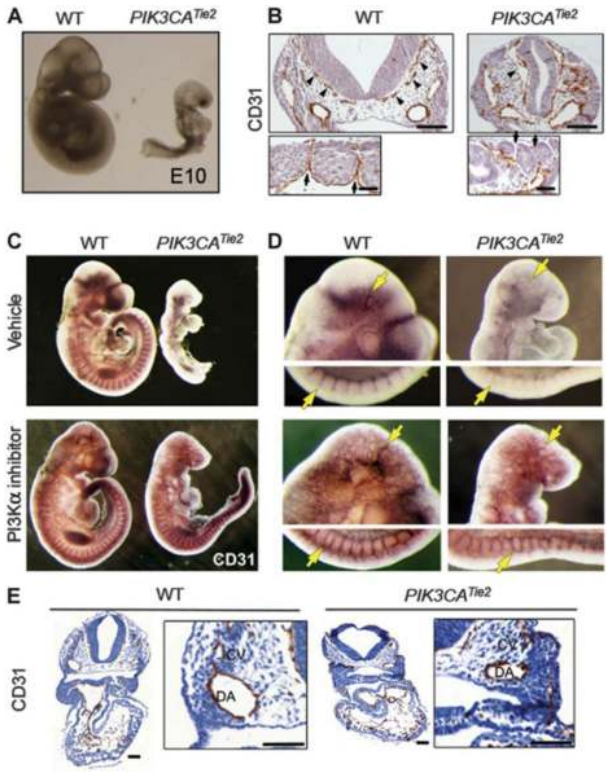

Fig. 5. *PIK3CA*^{H1047R} impairs embryonic angiogenesis

(**A**) Embryonic phenotype observed in *PIK3CA*^{WT} (left) and *PIK3CA*$^{Tie2\text{-}Cre}$ (right) littermates at E10. For morphological studies, a minimum of four dissections for each genotype were performed yielding $n \geq 15$ embryos. (**B**) CD31 staining of coronal sections from *PIK3CA*^{WT} and *PIK3CA*$^{Tie2\text{-}Cre}$ embryos at E9.5. Arrowheads indicate blood vessel enlargement defects in the meningeal vessels (upper panel), and arrows indicate the defects in the intersomitic vessels (lower panel). For CD31 histologic studies, a minimum of four embryos for each phenotype obtained from two different dissections were used. Scale bars, 100 μm. (**C**) Whole-embryo CD31 staining of *PIK3CA*^{WT} and *PIK3CA*$^{Tie2\text{-}Cre}$ embryos from mice treated with vehicle or PI3Kα inhibitor (BYL719, 50 mg kg^{-1}, daily, po; 48, 24, and 2 hours before embryos are harvested). For CD31 histologic studies, a minimum of four embryos for each condition were used. (**D**) Detailed view of the cephalic and intersomitic blood vessels from (C). Arrow indicates defects in the meningeal (upper panel) and the intersomitic vessels (lower panel). (**E**) CD31 coronal sections from embryos in (D). CV, cardinal vein; DA, dorsal aorta. Scale bars, 100 μm.